RQE Report: Analysis and Reconstruction Methods for Amplitude Sampling

Author: Hsin-Yu Lai
Supervisor: Alan V. Oppenheim

***Abstract*—Amplitude sampling is a recently proposed approach to representing an input signal by a sequence of continuous time instances and discrete amplitude values instead of a sequence of continuous amplitude values and discrete time instances as conventional time sampling. This representation can be promising when it is difficult to implement high-precision quantizers while the resolution of time can be sufficiently high. A better-known sampling technique exploiting such representation is level-crossing sampling, where continuous time instances are recorded whenever the input signal crosses a pre-defined set of levels. However, in contrast to time sampling, conditions for perfectly recovering a bandlimited signal based on level-crossing sampling are under-explored, except a special case – zero-crossing sampling, where only the level at zero is considered. Reconstruction methods for zero-crossing sampling nevertheless have been shown to lack stability and thus are subject to noise. Additional constraints on the input signals are needed to ensure stability. Most reconstruction methods for multi-level-crossing sampling on the other hand were developed in the context of data compression rather than perfect signal recovery.**

Since amplitude sampling can be defined as sampling a function transformed reversibly from the input signal, analysis on this reversible transformation facilitates potential perfect-reconstruction algorithms. Two algorithms for amplitude sampling are developed, the Bandlimited-Interpolation Approximation (BIA) and its iterative extension, the Iterative Amplitude Sampling Reconstruction (IASR). By relating amplitude sampling with nonuniform time sampling, we compare these algorithms with empirically the most efficient nonuniform time-sampling methods, the Voronoi method. Simulations show that not only does the BIA (same as the IASR with the first iteration) attain much higher signal-to-error ratio (SER) than the Voronoi method after the first iteration, but the IASR can generally reconstruct the original signal with fewer iterations than the Voronoi method.

***Index Terms*—Sampling theory, level-crossing sampling, nonuniform sampling and reconstruction, iterative algorithms.**

I. Introduction

Sampling theorems play an important role in signal processing as a connection between the analog world and digital processing. The most well-studied sampling theorem is the Shannon-Nyquist theorem [1], which formalizes a discrete representation of a bandlimited signal. It has profound impact on communication systems, the digital signal processing industry, and a great number of extensions have been proposed [2]–[4]. However, the Shannon-Nyquist sampling theorem and most of its extensions study a time-sampling framework, where a signal is represented by samples of continuous amplitude values and discrete time values; as a result, this framework assumes amplitude values can be measured in high resolution. However, when time rather than amplitude can be meausred in high resolution, one may consider representing the signal by samples of continuous time values and discrete amplitude values. An example is the level-crossing sampling technique [5], in which time values are recorded when the input signal crosses a specified set of amplitude values. A significant result in level-crossing sampling literature is Logan's theorem [6], which studies a specific class of level-crossing sampling – zero-crossing sampling, in which the level is set to be zero. The theorem provides sufficient conditions for reconstructing a signal under zero-crossing sampling. In [7], Petros showed that although Logan's theorem lacks stability guarantee, stability can typically be ensured with additional assumptions on sparsity. However, a more generalized theorem for level-crossing sampling with multiple levels is still under-explored. Most existing generalized level-crossing sampling methods focus on a low-power-consumption Analog-to-Digital Converter design [8]–[10]. They use zero-order hold to attain a piecewise-constant approximation of the original signal. Studies on more advanced signal reconstruction techniques are needed to improve this approximation.

This work studies a framework, referred to as amplitude sampling, recently proposed in [11]. This framework first adds a sufficiently large ramp to the input signal to make it monotonic. If we consider the amplitude of a signal as a function of time, the attained monotonic function allows time to be a function of amplitude. Amplitude sampling is then defined as uniformly sampling the amplitude of this transformed signal (i.e. uniformly sampling the function of amplitude) and thus acquiring a time sequence. Our goal is to recover the original signal from this time sequence. With this analytic definition of amplitude sampling, one may study the properties of the transformed signal and leverage these properties to develop a potentially theoretically more accurate reconstruction method than most multi-level-crossing sampling methods. We will also show that amplitude sampling can be algorithmically defined as shown in Figure 3, where a bounded saw-tooth like signal is added to the input signal and time is recorded whenever the resulting signal crosses a fixed level. This algorithmic definition enables a practical implementation of amplitude sampling.

To provide theoretical analysis, we will introduce the amplitude-time function, defined based on the transformed signal. Its properties in both the time domain and the frequency domain will be studied. With these properties, two reconstruction methods are developed: the bandlimited-interpolation approximation (BIA) and an iterative extension of the BIA, the iterative amplitude sampling reconstruction (IASR). Since the

samples are a series of nonuniform time instances, the original signal can also be reconstructed by a nonuniform sampling algorithm. By comparing the two developed algorithms with empirically the most efficient nonuniform sampling reconstruction algorithm, the Voronoi method [12], we show that in most simulation results, the IASR converges within fewer iterations than the Voronoi method. Moreover, parameters in the IASR can be designed to further improve the convergence rate.

II. Interpretations of Amplitude Sampling

A. Analytic Definition of an Amplitude-Time Function

In this section, we formalize the procedure of amplitude sampling. The key idea here is to leverage uniform time-sampling theorem. If we assume an input signal $g(t)$ strictly monotonic, then the inverse function $t(g)$ will also be strictly monotonic. Applying uniform level-crossing sampling on $g(t)$ is equivalent to uniformly "time"-sampling $t(g)$. If instead we assume the first derivatives of the input signal bounded, then we can transform an input signal to a monotonic function by adding a sufficiently large ramp. This procedure is described below:

$$y = g(t) = f(t) + \alpha t, \tag{1}$$

where we denote $f(t)$ as the input signal and $g(t)$ as the monotonic function, and α is chosen so that $g'(t) = f'(t) + \alpha > 0$ for all t[1]. Notice that the first derivative of a bandlimited signal with bandwidth W is bounded by $||f||_\infty W$ by Bernstein's inequality ($||\cdot||_\infty$ denotes the infinity norm). Therefore bandlimited signals satisfy the bounded-first-derivative assumption and a sufficiently large α can be found to attain a monotonic function $g(t)$. The variable y can be thought of as amplitude. The inverse function of $g(t) = y$ will be $g^{-1}(y) = t$, which is still a monotonic function. By subtracting $\frac{1}{\alpha}y$ from the inverse function, we define the amplitude-time function $h(y)$ as

$$h(y) = g^{-1}(y) - \frac{1}{\alpha}y. \tag{2}$$

This procedure is illustrated in Fig. 1. Notice that $h(y)$ is bounded if $f(t)$ is bounded since

$$\begin{aligned} h(f(t) + \alpha t) &= t - \frac{1}{\alpha}(f(t) + \alpha t) \\ &= -\frac{1}{\alpha}f(t). \end{aligned} \tag{3}$$

From Eq. (3), we obtain a relationship between f and h in a function-composition form [13]. Moreover, since α is chosen so that $g(t)$ is strictly monotonic and thus invertible, this relationship uniquely determines h from f.

A similar procedure can be applied to $h(y)$ to retrieve $f(t)$. The slope of the ramp is selected to be $1/\alpha$ so that the inverse function of $t = h(y)+y/\alpha$ is $g(t)$. After αt is subtracted from $g(t)$, $f(t)$ is recovered. Therefore another relationship between f and h can be formulated as

$$f(h(y) + \frac{1}{\alpha}y) = -\alpha h(y). \tag{4}$$

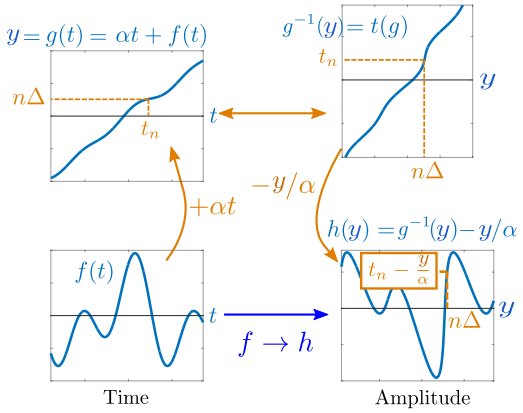

Fig. 1. The analytic definition of amplitude sampling (Figure adapted from [11])

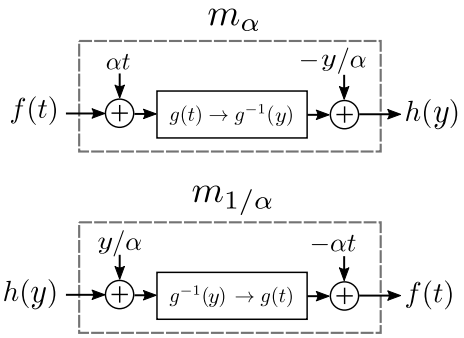

Fig. 2. Definition of the transformations m_α and $m_{1/\alpha}$ (Figure adapted from [11])

A similar argument can be made to show that Eq. (4) uniquely determines f from h. As a result, Eq. (3) and Eq. (4) describe two invertible transformations between f and h. As shown in Fig. 2, we denote these transformations as m_α and $m_{1/\alpha}$ respectively. Amplitude sampling is defined as a procedure to attain uniform samples $h(n\Delta)$ of $h(y)$. As a result, amplitude sampling can be realized by transforming f into h using the transformation m_α and uniformly sampling h to attain $h(n\Delta)$ as shown in Fig. 1. From Fig. 1 we also notice that there is a bijection between uniform samples $(n\Delta, h(n\Delta))$ on h and non-uniform samples $(t_n, f(t_n))$ on f determined by $t_n = h(n\Delta) + n\Delta/\alpha$ and $f(t_n) = -\alpha h(n\Delta)$. This observation allows us to recover f using a non-uniform sampling reconstruction algorithm which will be used for baseline comparison with our designed algorithms in Section VI.

B. Algorithmic Definition of Amplitude Sampling

Here we present an equivalent definition of amplitude sampling. As shown in Fig. 1, samples are taken whenever $f(t) + \alpha t$ crosses multiples of Δ. One can show that the attained time instances will not be changed if we subtract any

[1]We can also choose α such that $g'(t) = f'(t) + \alpha < 0$ for all t. Without lose of generality, in this work we will assume α is chosen to be positive and satisfy $g'(t) = f'(t) + \alpha > 0$.

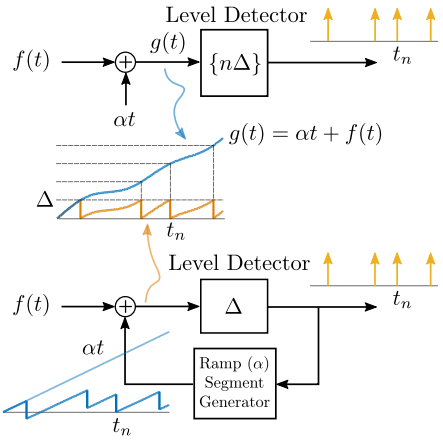

Fig. 3. The algorithmic definition of amplitude sampling (Figure adapted from [11])

multiples of Δ from $f(t) + \alpha t$ within any sample intervals. That is, for any $m, k \in \mathbb{Z}$, if we let

$$\tilde{g}(t) = \begin{cases} f(t) + \alpha t - m\Delta, & \text{if } t_k < t \leq t_{k+1}, \\ f(t) + \alpha t, & \text{otherwise,} \end{cases}$$

level-crossing sampling $\tilde{g}(t)$ at multiples of Δ will acquire the same time sequence $\{t_n\}$.

As a result, if we define a sawtooth-like signal $r(t)$ as

$$r(t) = \alpha t + m(t) \cdot \Delta, \tag{5}$$

where $m(t)$ is an integer-valued function such that $0 < r(t) + f(t) \leq \Delta$. Then by showing $m(t)$ does not change in any interval $(t_n, t_{n+1}]$, we know that level-crossing sampling $r(t)+f(t)$ will attain the same time instances as attained from level-crossing sampling $f(t) + \alpha t$. With these time instances, we can acquire the uniform samples of the amplitude-time function by calculating $h(n\Delta) = t_n - n\Delta/\alpha$. The block diagram for this sampling procedure is shown in Fig. 3, which can be an algorithmic definition of amplitude sampling that is equivalent to the analytic definition. Since the sawtooth-like signal $r(t)$ is bounded between $\Delta + A$ and $\Delta - A$ where A is the L^∞ norm of f, the block diagram provides a practical implementation of amplitude sampling. However, the analysis on amplitude sampling will be much simpler when we use the analytic definition. Therefore, in Section III and Section IV we will develop the time-domain properties and the frequency-domain properties of the amplitude-time functions by the analytic definition.

III. Time-Domain Properties of Amplitude-time Functions

In this section we present the relationship between f and h in the time domain. We first discuss the preservation of periodicity under the transformation m_α. By constraining $f(t)$ to be bandlimited and periodic, we know that $f(t)$ only contains finite number of frequency components. This simplification allows accessible simulation and might potentially help us analyze how harmonics interact after the transformation m_α. We then develop a matrix-based interpretation of m_α, from which several properties can be derived. Last but not least, we will depict $f(t)$ and $h(y)$ in the same figure and illustrate how we can use lines and intersections to find the value of one function from the other. Based on this illustration, an iterative implementation of m_α is derived. A theoretical proof of convergence will also be provided. We all also use this illustration to analyze how the distance between two functions changes after the transformation m_α. This analysis may be important for finding a theoretical proof for perfect reconstruction of amplitude sampling.

A. Periodicity

If $f(t)$ is periodic with a period T, i.e.

$$f(t+T) = f(t), \tag{6}$$

then the following can be obtained:

$$\begin{aligned} g(t+T) &= f(t+T) + \alpha(t+T) \\ &= f(t) + \alpha(t+T) \\ &= y + \alpha T, \end{aligned} \tag{7}$$

where $g(t) = f(t) + \alpha t = y$, and thus

$$t + T = g^{-1}(y + \alpha T). \tag{8}$$

From Eq. (8), we show that $h(y)$ is periodic with period αT:

$$\begin{aligned} h(y + \alpha T) &= g^{-1}(y + \alpha T) - \frac{1}{\alpha}(y + \alpha T) \\ &= t + T - \frac{1}{\alpha}(y + \alpha T) \\ &= g^{-1}(y) - \frac{1}{\alpha} y \\ &= h(y). \end{aligned} \tag{9}$$

Therefore periodicity is preserved under the transformation m_α and if $f(t)$ is periodic with a period T, then $h(y)$ is periodic with a period αT.

B. Matrix-based Properties

From Eq. (3) and Eq. (4), we notice that when f is fixed and α is increased, the corresponding function h shrinks in amplitude but expands in time. This effect can also be observed from the periodicity property, where the period in h is scaled by α. To normalize for these effects, we define the scaled amplitude-time function as

$$\tilde{h}(y) = -\alpha h(\alpha y). \tag{10}$$

From Eq. (10), a new relationship between $f(t)$ and $\tilde{h}(y)$ which we denote as $\tilde{m}_\alpha$ can be expressed as

$$\begin{aligned} f(y - \frac{1}{\alpha}\tilde{h}(y)) &= \tilde{h}(y). \\ \tilde{h}(t + \frac{1}{\alpha} f(t)) &= f(t). \end{aligned} \tag{11}$$

To avoid ambiguity, we add subscripts to each (scaled) amplitude-time function. That is, $h_{\alpha,f}(y)$ stands for $m_\alpha(f)(y)$ and $\tilde{h}_{\alpha,f}(y)$ stands for $\tilde{m}_\alpha(f)(y)$. One can check that with this normalization, we have $m_{1/\alpha} \circ m_\alpha(f) = f$ and $\tilde{m}_{-\alpha} \circ$

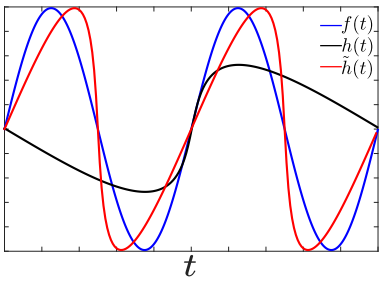

Fig. 4. Illustration of relationships among f, h, $\tilde{h}$

$\tilde{m}_\alpha(f) = f$. As shown in Figure 4, $\tilde{h}$ can be interpreted as a tilted f. Furthermore, from Eq. (11), as α goes to infinity, $\tilde{h}(t)$ approaches $f(t)$. Since $\tilde{h}$ is the scaled replica of h, as $\tilde{h}$ approaches the bandlimited function f, h intuitively will be more and more similar to a bandlimited function. This intuition will be strengthened by properties of the Fourier transform of h presented in Section IV.

The relationships in Eq. (11) can also be expressed in a matrix form as

$$\begin{bmatrix} y \\ \tilde{h}_{\alpha,f}(y) \end{bmatrix} = \begin{bmatrix} 1 & \frac{1}{\alpha} \\ 0 & 1 \end{bmatrix} \begin{bmatrix} t \\ f(t) \end{bmatrix}. \tag{12}$$

Note that with the normalization, the matrix-based representation of the transformation $\tilde{m}_\alpha$ forms a two-dimensional unitriangular group. This fact indicates the invertibility, commutability, and transitivity of the transformation. Moreover, the matrix form indicates that although the transformation between f and $\tilde{h}$ is not linear, the transformation between $(t, f(t))$ and $(y, \tilde{h}(y))$ is. In addition, we can use this matrix to analyze how time scaling and amplitude scaling on f affect $\tilde{h}$.

We first interpret time scaling and amplitude scaling on $f(t)$ in a matrix form. The scaled function $\tilde{f}(t) = Af(t/B)$ can be expressed as

$$\begin{bmatrix} \tilde{t} \\ \tilde{f}(\tilde{t}) \end{bmatrix} = \begin{bmatrix} B & 0 \\ 0 & A \end{bmatrix} \begin{bmatrix} t \\ f(t) \end{bmatrix}. \tag{13}$$

As a result, we could express the procedure of operating $\tilde{m}_\alpha$ to transform $\tilde{f}(t)$ into $\tilde{h}_{\alpha,\tilde{f}}(y)$ as

$$\begin{aligned} \begin{bmatrix} \tilde{y} \\ \tilde{h}_{\alpha,\tilde{f}}(\tilde{y}) \end{bmatrix} &= \begin{bmatrix} 1 & \frac{1}{\alpha} \\ 0 & 1 \end{bmatrix} \begin{bmatrix} B & 0 \\ 0 & A \end{bmatrix} \begin{bmatrix} t \\ f(t) \end{bmatrix} \\ &= \begin{bmatrix} B & 0 \\ 0 & A \end{bmatrix} \begin{bmatrix} 1 & \frac{A}{B\alpha} \\ 0 & 1 \end{bmatrix} \begin{bmatrix} t \\ f(t) \end{bmatrix} \\ &= \begin{bmatrix} B & 0 \\ 0 & A \end{bmatrix} \begin{bmatrix} y \\ \tilde{h}_{B\alpha/A,f}(y) \end{bmatrix}. \end{aligned} \tag{14}$$

From Eq. (14), we obtain:

$$\begin{aligned} \tilde{y} &= By. \\ \tilde{h}_{\alpha,\tilde{f}}(\tilde{y}) &= A\tilde{h}_{B\alpha/A,f}(y). \end{aligned} \tag{15}$$

Eq. (10) and Eq. (15) lead to:

$$\tilde{h}_{\alpha,\tilde{f}}(y) = A\tilde{h}_{B\alpha/A,f}(\frac{y}{B}). \tag{16}$$

$$\begin{aligned} \Rightarrow -\alpha h_{\alpha,\tilde{f}}(\alpha y) &= -B\alpha h_{B\alpha/A,f}(\frac{B\alpha}{A}\frac{y}{B}) \\ &= -B\alpha h_{B\alpha/A,f}(\frac{\alpha y}{A}). \end{aligned} \tag{17}$$

$$\Rightarrow h_{\alpha,\tilde{f}}(y) = Bh_{B\alpha/A,f}(\frac{y}{A}) \tag{18}$$

As a result, the amplitude-time function obtained from a scaled f can also be attained by scaling an amplitude-time function which is transformed from the unscaled f but with a scaled α. In fact, when $A = 1$, Eq. (18) becomes

$$h_{\alpha,\tilde{f}}(y) = Bh_{B\alpha,f}(y); \tag{19}$$

when $A = B$, Eq. (18) becomes

$$h_{\alpha,\tilde{f}}(y) = Bh_{\alpha,f}(y/B). \tag{20}$$

Eq. (19) shows how the corresponding amplitude-time function when the time in f is expanded by B can also be attained by operating the transformation with a scaled parameter $B\alpha$ on the original f and scaling the size of the resulting function. That is, up to a scale in size, an amplitude-time function can be attained from signals with different time scales (bandwidths). This observation intuitively tells us that it could be of similar difficulty between reconstructing a signal with a higher bandwidth and reconstructing a signal with a lower bandwidth if we choose the transformation parameter α correspondingly. On the other hand, Eq. (20) shows that when the ratio of the amplitude scaling factor A to the time expanding factor B is fixed, the corresponding amplitude-time function will be the same except that it will be scaled in time accordingly. This observation intuitively tells us that instead of changing the transformation parameter, we can maintain the difficulty when reconstructing a signal with a larger bandwidth by magnifying the signal and increasing the sampling rate. These two observations suggest that while conventional time-sampling theorems and reconstruction algorithms mostly relate with merely the bandwidth of a signal, both the amplitude of the signal and the transformation parameter α will affect the analysis of amplitude sampling. This discovery will be verified in the development of the frequency-domain properties of an amplitude-time function (see Section IV). We further develop a reconstruction algorithm that takes these extra parameters into consideration to achieve better performance (see Section VI).

We also explore the function space spanned by $\tilde{h}$ under the transformation $\tilde{m}_\alpha$. We observe that since the matrix-based representation of $\tilde{m}_\alpha$ belongs to the unitriangular matrix group, operating a sequence of $\tilde{m}_{\alpha_n}$ can be equivalent to operating a single transformation. That is,

$$\begin{aligned} \begin{bmatrix} y \\ \tilde{h}(y) \end{bmatrix} &= \begin{bmatrix} 1 & \frac{1}{\alpha_1} \\ 0 & 1 \end{bmatrix} \begin{bmatrix} 1 & \frac{1}{\alpha_2} \\ 0 & 1 \end{bmatrix} \cdots \begin{bmatrix} 1 & \frac{1}{\alpha_n} \\ 0 & 1 \end{bmatrix} \begin{bmatrix} t \\ f(t) \end{bmatrix} \\ &= \begin{bmatrix} 1 & \frac{1}{\alpha_1} + \frac{1}{\alpha_2} + \cdots + \frac{1}{\alpha_n} \\ 0 & 1 \end{bmatrix} \begin{bmatrix} t \\ f(t) \end{bmatrix}. \end{aligned} \tag{21}$$

In other words, composing $\tilde{m}_\alpha$ does not expand the function space spanned by functions generated from $\{t, f(t)\}$ using $\tilde{m}_\alpha$. We notice that $f(t)$ is also in this space. Moreover, one may be able to develop an algorithm to modify the amplitude-time function when α is not accurate by composing transformations. However, this idea is still unexplored.

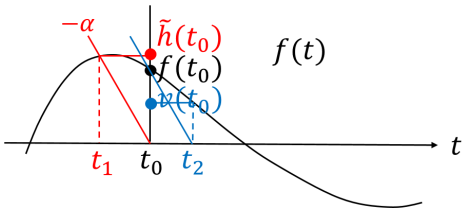

Fig. 5. Determination of the value $\tilde{h}(t_0) = f(t_0 - \frac{1}{\alpha}h(t_0))$ and the value $v(t_0) = f(t_0 + \frac{1}{\alpha}f(t_0))$ from the plot of $f(t)$.

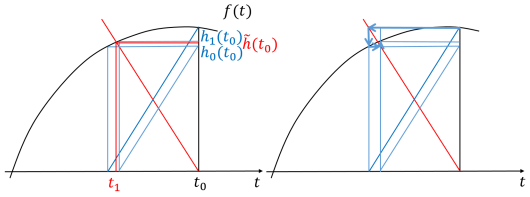

Fig. 6. An illustration of how the value $h_n(t_0) = f(t_0 - \frac{1}{\alpha}h_{n-1}(t_0))$ approaches $\tilde{h}(t_0)$ through iterations.

C. Implementation of m_α

Before showing the implementation of the transformation m_α, we first give an illustration of the transformation $\tilde{m}_\alpha$.

From Eq. (11), we observe that finding $\tilde{h}(t_0)$ is equivalent to finding t_1 such that $t_0 = t_1 + \frac{1}{\alpha}f(t_1)$ and then taking the value $f(t_1)$ as $\tilde{h}(t_0)$. As shown in Figure 5, t_1 can be determined by drawing a line with a slope $-\alpha$ through $(t_0, 0)$. With the knowledge of t_1, the value $\tilde{h}(t_0) = \tilde{h}(t_1 + \frac{1}{\alpha}f(t_1)) = f(t_1)$ can be measured as indicated in the plot.

The same idea can be applied to other function-composition forms. For example, as shown in Fig. 5, the value $v(t_0) = f(t_0 + \frac{1}{\alpha}f(t_0))$ can be observed by drawing a line with slope $-\alpha$ through $(t_0, f(t_0))$, since this line finds the value $t_2 = t_0 + \frac{1}{\alpha}f(t_0)$. Figure 5 also shows that $\tilde{h}(t_0)$ is obtained by finding a value before time t_0 while $v(t_0)$ is obtained by finding a value after time t_0. Therefore, instead of finding $f(t_0 + \frac{1}{\alpha}f(t_0))$, we pursue the value $h_0(t_0) = f(t_0 - \frac{1}{\alpha}f(t_0))$, which can be shown in Figure 6.

Now we iteratively update our approximation of $\tilde{h}$ by composing f with the function obtained from the last iteration. As shown in Figure 6, if f is composed with $t - \frac{1}{\alpha}h_0(t)$, the value $h_1(t_0) = f(t_0 - \frac{1}{\alpha}h_0(t_0))$ can still be observed in the plot of f. Moreover, the iteration $h_{n+1}(t_0) = f(t_0 - \frac{1}{\alpha}h_n(t_0))$ appears to converge to $\tilde{h}(t_0)$, where n denotes the index of the iteration. We now prove in the following theorem that not only such iteration uniquely converges to $\tilde{h}(t)$, its convergence rate can also be determined.

Theorem 1: The function $h_{n+1}(t) = f(t - \frac{1}{\alpha}h_n(t))$ will converges linearly to $h(t)$ where $h = m_\alpha(f)$ if $\lambda = \sup \frac{|f'(t)|}{|\alpha|} < 1$; in such case λ is the convergence rate.

Proof 1: We recognize that as n goes to infinity the second equation of Eq. (11) and the iteration $h_{n+1}(t) = f(t - \frac{1}{\alpha}h_n(t))$ become the same if the limit exists. Moreover, Figure 6 suggests an explanation by the fixed-point theorem [14]. We first re-formulate the problem as finding t_1 such that

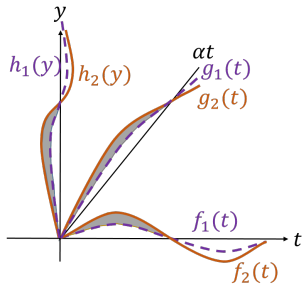

Fig. 7. Illustration of L^1 difference between f_1 and f_2 and between h_1 and h_2. The gray areas in the figures have the same size.

$t_1 = t_0 - \frac{1}{\alpha}f(t_1) := p_{t_0}(t_1)$. If $p_{t_0}(t)$ satisfies the Lipschitz condition [15], i.e.

$$|p_{t_0}(a) - p_{t_0}(b)| \leq \lambda |a - b| \tag{22}$$

for some $|\lambda| < 1$, where $\lambda = \sup \frac{|f'(t)|}{\alpha}$, then the iteration will uniquely converge to the fixed point $p_{t_0}(t_1) = t_1$. Since $g(t)$ is required to be invertible, which implies $f'(t) + \alpha > 0$ for all t, we only need to add a constraint on the positive derivative of $f(t)$ to ensure that $\alpha > sup|f'(t)|$ so that $|\lambda| < 1$ can be satisfied. By the fixed-point theorem, we also observe that the algorithm is of linear convergence with a convergence rate λ. Since λ decreases as α increases, it shows that the algorithm can converge faster with a larger α.

D. Distance between Two Functions

In this section, we analyze how the distance between two functions translates to the distance between their corresponding amplitude-time functions. That is, if we let $h_1 = m_\alpha f_1$ and $h_2 = m_\alpha f_2$, we want to find β and γ such that $\beta\|f_1 - f_2\| \leq \|h_1 - h_2\| \leq \gamma\|f_1 - f_2\|$. Figure 7 illustrates that β and γ for the L^1 norm is one, since the area between f_1 and f_2 is the same as the area between g_1 and g_2 where $g_i(t) = f_i(t) + \alpha t$, the area between h_1 and h_2 is the same as the area between g_1^{-1} and g_2^{-1} where $g_i^{-1}(y) = h_i(y) + \frac{1}{\alpha}y$, and the difference between g_1 and g_2 defines the same area as the difference between g_1^{-1} and g_2^{-1}.

Figure 8 on the other hand illustrates how to find β and γ for the L^∞ norm. As shown in Figure 5, we can determine $\tilde{h}(t)$ by finding the intersection between $f(t)$ and a line. As a result, the absolute difference between $\tilde{h}_1(t)$ and $\tilde{h}_2(t)$ can be shown to be the length of the red vertical line in Figure 8(a). We also know that there is a 1-1 correspondence between t_0 and t_1 and between t_0 and t_2. Figure 8(b) shows that given a t_1 where a line drawn from $(t_0, 0)$ intersects with $\tilde{h}_1$ and given a t_2 where that line intersects with $\tilde{h}_2$, f_1 can only be between the two black lines due to mean value theorem and

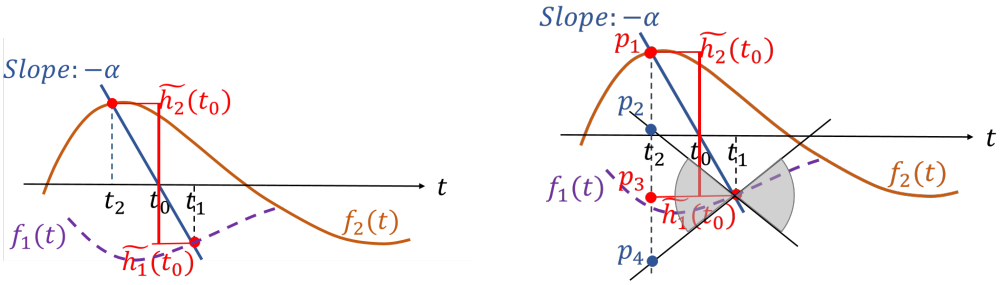

Fig. 8. (a) Illustration of finding $\tilde{h}_1(t_0)$ and $\tilde{h}_2(t_0)$ from $f_1(t)$ and $f_2(t)$; (b) The gray areas indicate where $f_1(t)$ can lie. As a result, $f_1(t_2)$ needs to locate between p_2 and p_4. That is, the absolute difference between $f_1(t_2)$ and $f_2(t_2)$ is bounded by the distance between p_1 and p_2 and that between p_1 and p_4. The distance between p_1 and p_3 is the same as the absolute difference between $\tilde{h_1}(t_0)$ and $\tilde{h_2}(t_0)$. Then we can use the difference between $f_1(t_2)$ and $f_2(t_2)$ to bound the difference between $\tilde{h_1}(t_0)$ and $\tilde{h_2}(t_0)$.

the Bernstein inequality. As a result, we have the followings:

$$\begin{aligned}
&\frac{\alpha}{\alpha+A\sigma}|f_1(t_2)-f_2(t_2)| \le |\tilde{h}_1(t_0)-\tilde{h}_2(t_0)|,\\
&|\tilde{h}_1(t_0)-\tilde{h}_2(t_0)| \le \frac{\alpha}{\alpha-A\sigma}|f_1(t_2)-f_2(t_2)|\\
\Rightarrow&\frac{\alpha}{\alpha+A\sigma}|f_1(t_2)-f_2(t_2)| \le \|\tilde{h}_1-\tilde{h}_2\|_\infty,\\
&|\tilde{h}_1(t_0)-\tilde{h}_2(t_0)| \le \frac{\alpha}{\alpha-A\sigma}\|f_1-f_2\|_\infty\\
\Rightarrow&\frac{\alpha}{\alpha+A\sigma}\|f_1-f_2\|_\infty \le \|\tilde{h}_1-\tilde{h}_2\|_\infty \le \frac{\alpha}{\alpha-A\sigma}\|f_1-f_2\|_\infty\\
\Rightarrow&\frac{1}{\alpha+A\sigma}\|f_1-f_2\|_\infty \le \|h_1-h_2\|_\infty \le \frac{1}{\alpha-A\sigma}\|f_1-f_2\|_\infty,
\end{aligned} \tag{23}$$

where the second to the last equation follows from the 1-1 mapping of t_0 and t_2.

IV. Frequency-Domain Properties of Amplitude-time Functions

In this section, we discuss the frequency-domain properties of amplitude-time functions. Recall that our goal is to recover f from uniform samples of h. If h is bandlimited, f can be reconstructed by applying bandlimited interpolations on the samples $h(n\Delta)$ and using the transformation $m_{1/\alpha}$ to retrieve f. However, in this section, we will show that f and h cannot both be bandlimited unless they are constants.[2] Therefore, if we assume f to be bandlimited, the resulting function attained from the previous procedure will not be bandlimited and thus will be different from f. Nevertheless, the Fourier transform of h is shown to exponentially decay in frequency [11]. A sketch of the proof is provided.[3] These properties indicate that if f is bandlimited, although an amplitude-time function generally cannot be reconstructed from its uniform amplitude samples by bandlimited interpolation, the aliasing introduced from sampling h can be negligible if the sampling rate is sufficiently high.

[2] [11] provides a different proof.

[3]The sketch of the proof presented in this work is not complete and is different from the proof presented in [11]. Please refer to [11] for a complete proof of the theorem.

A. Bandlimitedness

Here we prove that $h(y)$ is not bandlimited unless $f(t)$ is a constant by contradiction as the following.

Theorem 2: For any $\alpha \neq 0$, the amplitude-time function $h = m_\alpha(f)$ and f cannot be both bandlimited unless they are constant functions.

Proof 2: If $h(y)$ is bandlimited, $h(y)$ can be analytically extended to the entire complex plane and becomes an entire function of order one [16]. Since f is assumed to be bandlimited, after analytic extension, $f(t)$ and $f(t)+\alpha t$ are also entire functions of order one. Moreover, since the composition of two entire functions remains an entire function, a function $u(z) = h(f(z)+\alpha z)$ will be entire if h is entire (z is any complex number). From Eq. (3), we know that $u(z)|_{z\in\mathbb{R}} = -\frac{1}{\alpha}f(z)$. Since both $h(f(z)+\alpha z)$ and $-\frac{1}{\alpha}f(z)$ are analytic on the whole complex plane and the values on the real line of $h(f(z)+\alpha z)$ and $-\frac{1}{\alpha}f(z)$ are the same, by analytic continuation[4], it implies that $h(f(z)+\alpha z) = -\frac{1}{\alpha}f(z)$ for all $z \in \mathbb{C}$. However, from [18], if $h(f(z)+\alpha z)$ is an entire function of a finite order and both h and f are entire functions, then either $f(z)$ is polynomial or $h(z)$ is of order zero. Since we assume $h(z)$ to be an entire function of order one, we remove the second possibility. Since $f(z)$ is bandlimited, $f(z)$ being polynomial will imply it to be a constant function. Therefore, $h(z)$ is bandlimited if and only if $f(z)$ is a constant. In such case h is also a constant.

B. Decay Rate in the Frequencies

Although $h(y)$ is not bandlimited in general, it is shown in [11] that its Fourier transform exponentially decays as frequency increases. In this section, we present a sketch of the proof which is somewhat different from that in [11]. Notice that in this section we will let both y and t be complex variables. From [16], we have the following theorem:

Theorem 3: **[16]** The Fourier transform of $h(y)$ exponentially decays, i.e. $\hat{h}(\xi)e^{\sigma|\xi|} \in L_2$, if and only if the following two conditions are satisfied:

(a) $h(y)$ can be analytically extended in a strip $|\Im\{y\}| < \sigma$.

[4]The theorem of analytic continuation can be found in most complex analysis book, e.g. [17].

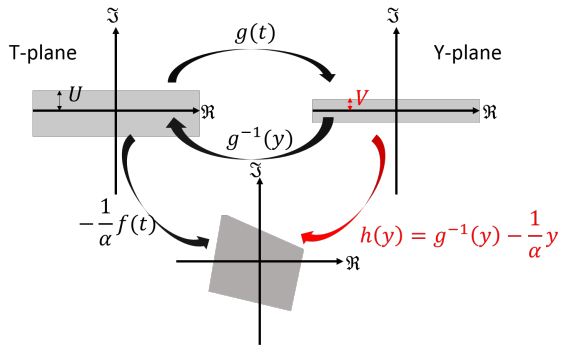

Fig. 9. The strip U and the strip V defined the open space where $g(t)$ and $g^{-1}(y)$ are locally invertible respectively. The strip V then determines the decay rate of the Fourier transform of the amplitude-time function h.

(b) $\|h(y)\|_\infty \leq C$ uniformly in the strip for some constant C.

Here $\hat{h}(\xi)$ is the Fourier transform of h with ξ being the radial frequency. The variable y is a complex number and thus can be written as $y = y_1 + iy_2$ where $y_1, y_2 \in \mathbb{R}$, and $\Im\{y\} = y_2$.

In this section, we outline a procedure to show (a). From Eq. (3), Fig. 9 is obtained. If we can find a strip with a width $V > 0$ where g^{-1} is well-defined and analytic,[5] then $h(y) = g^{-1}(y) - \frac{1}{\alpha}y$ is analytic in a strip with the width V, which satisfies (a). By (a) the width will indicate the decay rate of the Fourier transform of h.

From the Inverse Function Theorem [17], if $g'(t) \neq 0$, $g(t)$ is locally injective. However, locally injective generally cannot imply globally injective; $g(t)$ is required to be globally injective on the preimage of the strip in the Y-plane to ensure g^{-1} to be well-defined in the strip. Here we only show a method to determine a region in the Y-plane where g^{-1} can be locally well-defined and thus h is locally well-defined. A proof to show $h(y)$ is well-defined in the strip, i.e. $g(t)$ is globally injective on the preimage of the strip in the Y-plane, can be found in [11]. Since h is continuous and the boundary is mapped to the boundary by Open Mapping Theorem [17], a lower bound of the width of the strip can be found in the Y-plane.

If the bandwidth of $f(t)$ is smaller than W, by Bernstein's inequalities [19], we have

$$|f(t)| \leq \|f\|_{C(\Re)} e^{W|\Im\{t\}|}, \tag{24}$$

and

$$|f'(t)| \leq W\|f\|_{C(\Re)} e^{W|\Im\{t\}|}, \tag{25}$$

where $\|f\|_{C(\Re)}$ refers to the infinity norm when f is restricted to the real line. Then without lost of generality if we assume α is sufficiently large, we can derive the followings:

$$\begin{aligned} g'(t) &= f'(t) + \alpha. \\ |g'(t)| &\geq \big|\, |f'(t)| - |\alpha| \,\big| \\ &\geq \alpha - W\|f\|_{C(\Re)} e^{W|\Im\{t\}|} \\ &= \alpha - AWe^{W|\Im\{t\}|}, \end{aligned} \tag{26}$$

where we let $A = \|f\|_{C(\Re)}$.

From Eq. (25) we know if

$$|\Im\{t\}| \leq \frac{1}{W} \log \frac{\alpha}{AW}, \tag{27}$$

then

$$\begin{aligned} |f'(t)| &\leq AWe^{W|\Im\{t\}|} &(28)\\ &\leq \alpha. &(29) \end{aligned}$$

Then from Eq. (26) we know that for any t satisfying Eq. (27), $g'(t) \neq 0$. Therefore, $g(t)$ is locally injective in a strip with width $|U| = \frac{1}{W} \log \frac{\alpha}{AW}$. To determine V, we need to find $V = \min_{|\Im\{t\}|=U} |\Im\{g(t)\}|$. By Eq. (24),

$$\begin{aligned} |\Im\{g(t)\}| &\geq \big| - |\Im\{f(t)\}| + |\Im\{\alpha t\}| \,\big| \\ &\geq -Ae^{W|U|} + \alpha|U| \\ &= \frac{\alpha}{W} \log \frac{\alpha}{AW} - \frac{\alpha}{W} \\ &= V, \end{aligned} \tag{30}$$

since $|\Im\{t\}| \leq U$.

From Eq. (30), we obtain a conjecture:

Conjecture 1: The Fourier transform of $h(y)$ exponentially decays, i.e. $\hat{h}(\xi)e^{\sigma|\xi|} \in L_2$ where h is the amplitude-time function transformed with a transformation parameter α from a function with a bandwidth W and $\sigma = \frac{\alpha}{W} \log \frac{\alpha}{AW} - \frac{\alpha}{W}$ where $A = \|f\|_{C(\Re)}$.

It turns out the decay rate shown in Eq. (30) is slightly smaller than the following theorem.

Theorem 4: **[11]** The Fourier transform of $h(y)$ exponentially decays, i.e. $\hat{h}(\xi)e^{\sigma|\xi|} \in L_2$ where h is the amplitude-time function transformed with a transformation parameter α from a function with a bandwidth W and $\sigma = \frac{\alpha}{W} \log \frac{\alpha}{AW} - \frac{\alpha - AW}{W}$ where $A = \|f\|_{C(\Re)}$.

The difference between the conjecture and the theorem is caused by how many orders of the Bernstein's ineuqalities are used. Only the zeroth and the first order of the Bernstein's inequalities are utilized in the conjecture. [11] used more orders of Bernstein's inequalities to show global invertibility and determine the decay rate. However, after h is scaled as in Eq. (10), the decay rate shown in Eq. (30) and the decay rate shown in [11] will be the same as α goes to infinity. As discussed in Section III, intuitively h will become more like a bandlimied function as α increases. This theorem supports this intuition by showing the decay rate will increase with a larger α. It is also interesting to notice that the decay rate is dependent on the amplitude of f. As discussed in Section III, when dealing with a function with a larger bandwidth, by shrinking the amplitude f correspondingly, we are able to attain the same amplitude-time function except with a scale in time. This observation is supported by the factor AW in the theorem.

V. Reconstruction

In this section, we explore methods to recover a bandlimited function f from samples of its amplitude-time function. The first algorithm, the Bandlimited-Interpolation Approximation (BIA), approximates $h(y)$ by the bandlimited interpolation of

[5] Y-plane denotes the complex-plane extension of y and T-plane denotes the complex-plane extension of t.

Fig. 10. The block diagram for the Bandlimited-interpolation approximation (BIA) algorithm

$h(n\Delta)$ and transforms the resulting approximate amplitude-time function $\breve{h}(y)$ into the approximate signal $\breve{f}(t)$ by the transformation $m_{1/\alpha}$. Another reconstruction algorithm, the Iterative Amplitude Sampling Reconstruction (IASR), iteratively keeps the approximate signal in each iteration bandlimited and updates the approximation regarding the difference between samples of its amplitude-time function and the samples $h(n\Delta)$.

Nonuniform time-sampling reconstruction algorithms can also be used to reconstrct f. As discussed in Section II, each sample $(n\Delta, h(n\Delta))$ can be bijectively mapped to a point $(t_n, f(t_n))$ in f. Therefore, other than reconstructing f directly from the uniform samples of h, an alternative is to first map the uniform samples of h to the nonuniform samples of f and then implement nonuniform time-sampling reconstruction methods. Since our proposed algorithm is iterative, it is reasonable to compare our performance with an iterative nonuniform time-sampling reconstruction algorithm. Moreover, since the Voronoi method was shown to perform the best in numerical results [12], we compare our algorithms with the Voronoi method. The simulation result will be presented in Section VI.

A. Bandlimited Interpretation Approximation (BIA)

We first approximate $h(y)$ by the bandlimited interpolation of its uniform samples $\{h(n\Delta)\}$. However, since the bandlimited-interpolation function $\breve{h}(y)$ by definition is bandlimited, it cannot be the same as $h(y)$ as discussed in Section IV. Nevertheless, according to [11], $\|\breve{h}(y)-h(y)\|_\infty \leq Ce^{-\frac{\sigma}{\Delta}}$ for some constant $C > 0$ where $\sigma = \frac{\alpha}{W}\log(\frac{\alpha}{AW}) - \frac{\alpha - AW}{W}$. That is, the error measured in the L_∞ norm between $\breve{h}(y)$ and $h(y)$ decreases exponentially fast as $1/\Delta$ increases. We then use $\breve{f}(t)$, the function transformed from $\breve{h}(y)$ by $m_{1/\alpha}$, as the resulting approximation of $f(t)$. Similarly, $\breve{f}(t)$ cannot be the same as $f(t)$ since $\breve{f}(t)$ will not be bandlimited.[6]

B. Iterative Amplitude Sampling Reconstruction (IASR)

As discussed in the previous section, the BIA cannot perfectly recover the original signal because the resulting function $\breve{f}(t)$ is not bandlimited. This observation suggests processing $\breve{f}(t)$ through a low-pass filter to attain a bandlimited approximation $\breve{f}_0(t)$. Since the values of the samples $h(n\Delta)$ are known, we can further transform $\breve{f}_0(t)$ back to the amplitude domain by m_α and re-sample it to obtain $\{\breve{h}_0(n\Delta)\}$. Since $\{\breve{h}_0(n\Delta)\}$ are not the same as $\{h(n\Delta)\}$, this suggests an iterative algorithm in which $\breve{h}_0(n\Delta)$ is subtracted from $h(n\Delta)$ and the error samples $e_{h,1}(n\Delta) = \breve{h}_0(n\Delta) - h(n\Delta)$ are interpolated and transformed to obtain $e_{f,1}(t)$ and then is added back to $\breve{f}_0(t)$. The iteration process is summarized in Figure 11.

We show in the Appendix that if the IASR converges, perfect reconstruction can be ensured if the sampling rate $1/\Delta$ is higher than $W/(\alpha\pi)$. However, to analyze whether the IASR converges, we cannot emulate the conventional analysis on iterative nonuniform sampling algorithms as outlined in Proposition 1 (see Appendix). As shown in Figure 11, our iteration can be formulated as $f_{k+1} = f_k + B(h - m_\alpha f_k) = f_k + B(m_\alpha f - m_\alpha f_k)$. It is different from $f_{k+1} = f_k + A(f - f_k)$ as in Eq. (40). A way to prove the convergence of the IASR is to show $\|B(m_\alpha f - m_\alpha f_k)\| \leq \|B\|\|m_\alpha f - m_\alpha f_k\| < \gamma\|f - f_k\|$ for some $\gamma < 1$. The operator B consists of a bandlimited interpolation, a low-pass filtering, and an $m_{1/\alpha}$ transformation. While it is easier to analyze how bandlimited interpolation and low-pass filter affects the L^2 norm, so far we can only show how m_α affects L^1 norm and the L^∞ norm as discussed in Section III. The nonlinearity of m_α makes it difficult to analyze the L^2 norm of $\|m_\alpha f - m_\alpha f_k\|$ and therefore whether the IASR converges remains open. However, the simulation results in Section VI suggest that the IASR algorithm converges as long as $1/\Delta > W/(\alpha\pi)$.

C. Voronoi Method

As discussed in Section II , there is a bijection between $(y, h(y))$ and $(t, f(t))$. With the knowledge of α, we can correspond $\{(n\Delta, h(n\Delta))\}$ to $\{(t_n, f(t_n))\}$ by letting $t_n = h(n\Delta) + n\Delta/\alpha$ and $f(t_n) = -\alpha h(n\Delta)$. As a result, we can use non-uniform reconstruction algorithm to recover f based on $\{(t_n, f(t_n))\}$. Here we chose the Voronoi method since it is studied to empirically converge to the original signal with the fastest rate. Figure 12 shows the block diagram for the Voronoi method. The rate and the proof of convergence can be found in the Appendix.

VI. Simulation Results

In this section, we compare the performance of the BIA, the IASR, and the Voronoi algorithms on randomly generated bandlimited signals based on their signal-to-error ratio (SER) defined as:

$$SER(dB) = 10\log_{10}\left(\frac{||f||_2^2}{||f - \breve{f}||_2^2}\right), \tag{31}$$

where $\breve{f}$ denotes the reconstructed signal.

The effects of three parameters are evaluated – the transformation parameter α, the sampling interval Δ, and the bandwidth of the original signal W. Details of the generation of the bandlimited signals can be found in [20]. Since the approximate signal from the BIA method and that from the first iteration of the IASR method only differ in whether the signal is processed by a low-pass filter, their corresponding SER values are similar. As a result, in the figure we only show the SER of the IASR and the Voronoi method measured in each iteration.

[6]It should be noticed that $\breve{h}(y) + y/\alpha$ should be invertible. This would affect the range of Δ we can choose when we implement amplitude sampling. A necessary and sufficient condition on Δ has not yet been found to ensure the invertibility. Moreover, the error bound between $f(t)$ and $\breve{f}(t)$ is still unknown.

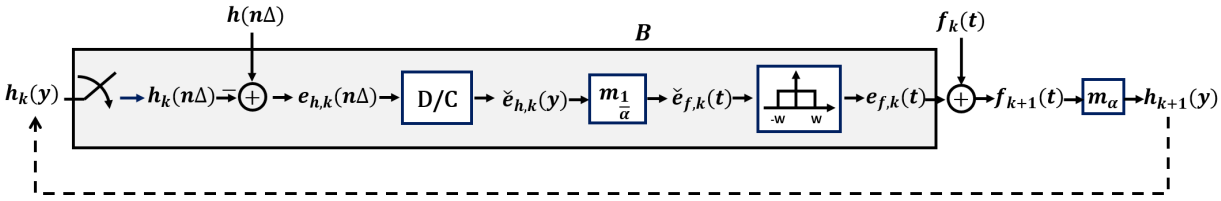

Fig. 11. The block diagram for the Iterative Amplitude Sampling Reconstruction (IASR) algorithm. The variable k denotes the kth iteration.

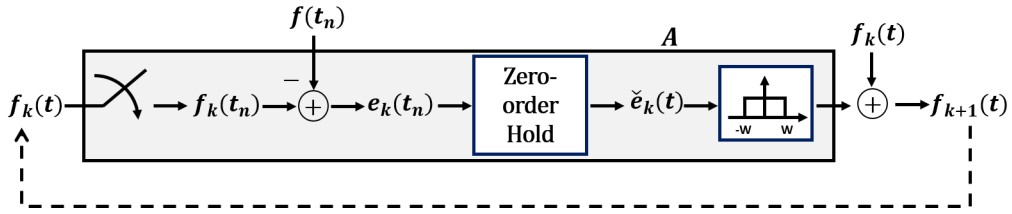

Fig. 12. The block diagram for the Voronoi method. The variable k denotes the kth iteration.

From Fig. 13, we observe that generally the IASR algorithm achieves higher SER than the Voronoi method in the first iteration. Moreover, the IASR converges faster than the Voronoi method. The difference in the convergence rate is particularly substantial when the sampling rate is closer to the Nyquist sampling rate.

When α increases, Δ decreases, or W decreases, the convergence rates of both the IASR and the Voronoi methods increase. Furthermore, the SER measured after the first iteration of the IASR also increases with these changes while the SER measured after the first iteration of the Voronoi method hardly changes. The effects of these parameters on the IASR can be intuitively explained by Theorem 4. Since the exponential decay rate of the amplitude-time function in frequency grows as α increases or W decreases, the aliasing effect introduced by the bandlimited approximation is reduced.[7] The size of Δ on the other hand determines how much area outside the sampling frequency will be. With a smaller Δ, the area outside $1/\Delta$ will be smaller[8] and thus the amount of aliasing can be reduced. By reducing the error introduced by the aliasing effect, the performance of the IASR will be improved in each iteration.

The effects of these parameters on the convergence rate of the Voronoi method on the other hand can be explained by the theoretical convergence rate discussed in the Appendix. However, since the approximation of the Voronoi method after the first iteration is based on the zero-order hold, these parameters can hardly affect the performance of the Voronoi method after the first iteration.

Since the average sampling rate of f is α/Δ, we would also like to evaluate the effect of α when the sampling rate is fixed. Fig. 14 shows that we can improve the convergence rate by increasing α, this observation can as well be intuitively explained by the reduction in the aliasing effect of the bandlimited approximation since while $(\alpha|\xi|)/W$ is fixed, the convergence rate shown in Theorem 4 will still be affected by how α and AW differ. As a result, the design parameter α allows us to potentially speed up the convergence while keeping the sampling rate on the original signal. Since the IASR exploits the properties of the amplitude sampling, particularly the exponential decay rate of the Fourier transform of the amplitude-time function, while the Voronoi method was not developed for amplitude sampling and thus does not assume any sampling method, it is reasonable that in general the IASR attains a substantially larger convergence rate and achieves better approximation after the first iteration.

[7]This explanation nonetheless needs further analysis because the exponential decay can only apply to sufficiently large frequencies.

[8]This explanation also assumes that $1/\Delta$ is sufficiently large and therefore the exponential decay can be applied.

VII. Conclusion

In this work, we studied amplitude sampling, a recently proposed method to represent signals by continuous-time- and discrete-amplitude-valued samples rather than by discrete-time- and continuous-amplitude-valued samples as conventional time-sampling techniques. Since amplitude sampling can be defined by uniformly sampling the amplitude-time function, which is transformed from the input signal using a reversible transformation, m_α, by studying properties of this amplitude-time function, we can develop reconstruction approaches that leverage these properties and due to the reversibility may potentially perfectly recover the input signal. In this work, properties of an amplitude-time function in both the time domain and in the frequency domain were examined. Based on these properties, we developed two reconstruction algorithms, the Bandlimited Interpolation Approximation (BIA) and its iterative extension, the Iterative Amplitude Sampling Reconstruction (IASR), and compared them with empirically the most efficient non-uniform sampling algorithm, the Voronoi method. We showed that the IASR not only outperformed the Voronoi by attaining much better approximation after the first iteration and achieving much larger convergence rate, it also allows further improvement on the convergence rate by changing the transformation parameter α without changing the sampling rate. Two conference papers are published based on these results [21], [22].

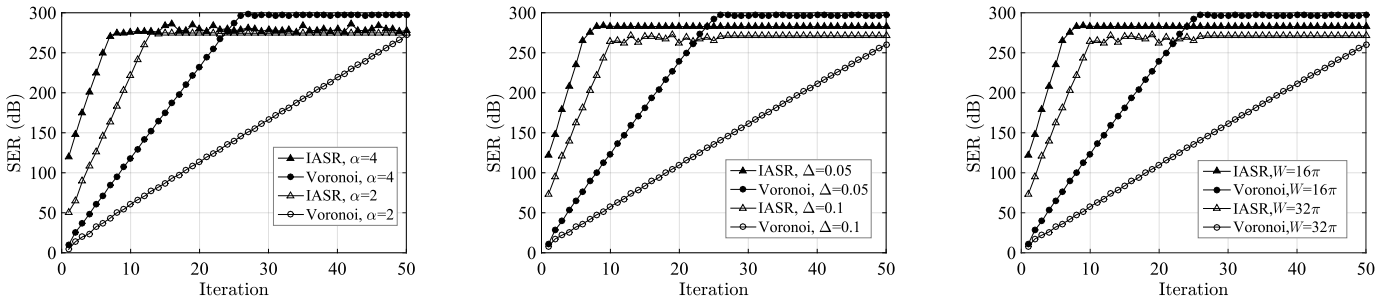

Fig. 13. Comparison on how the performance of the IASR and the Voronoi method change with different α, Δ, and W.

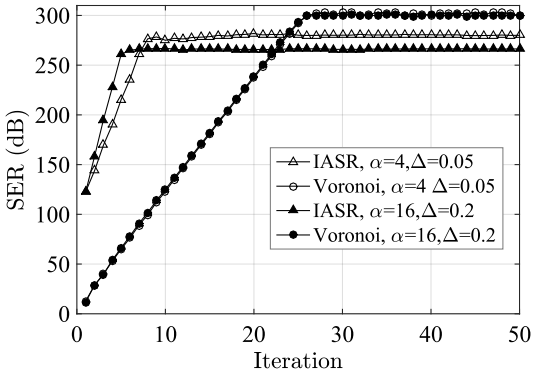

Fig. 14. Comparison on how the performance of the IASR and the Voronoi method change with different α but a fixed sampling rate.

APPENDIX A
BACKGROUND ON UNIQUENESS SEQUENCE AND SAMPLING SEQUENCE

Here we provide some background that will be useful later.

A uniqueness sequence is defined as follows:

Definition 1: **[23], [24]** The set of points $\{t_n\}$ is a uniqueness sequence for $\mathcal{B}(S)$ if there are no two different functions $f, g \in \mathcal{B}(S)$ that agree in $\{t_n\}$.

The notation $\mathcal{B}(S)$ denotes the space of square integrable signals with a finite support S in the frequency domain. It is clear that if two different functions $f(t)$ and $g(t)$ with the same support in frequency agree at $t = \{t_n\}$, then we cannot reconstruct both f and g based on these samples without any other assumption. That is, $\{f(t_n)\}$ can be a representation of $f(t)$ in $\mathcal{B}(S)$ if and only if $\{t_n\}$ is a uniqueness sequence.

The idea of representing a signal by its nonuniform sampling can be traced back to Cauchy as stated in Black's paper [25]. Black also discussed scenarios where nonuniform sampling is encountered, for example, random sampling for nonsynchronous multiplexing [25]. They stated possible conditions for a uniqueness sequence for a bandlimited-signal space. These conditions were later proved by [26], [27] in the following theorem:

Theorem 5: **[26]** If the average sampling rate of the nonuniform samples $(t_n, f(t_n))$ is higher than the Nyquist rate $m(S)/(2\pi)$ where $m(S)$ denotes the measure of S, the nonuniform samples can uniquely represent a bandlimited signal. That is, $\{t_n\}$ is a uniqueness sequence.

A more rigorous statement can be found in [27], in which Beutler also proved the theorem but in a more general mathematical setting.

However, Theorem 5 is not useful in practice since it does not imply how a finite-energy perturbation on samples affects the reconstructed signal. The resulting error can be unbounded. In reality we can hardly design an algorithm with infinite precision and no error introduced. The definition of a sampling sequence was established to resolve this issue:

Definition 2: **[23]** The set of points $\{t_n\}$ is a sampling sequence for $\mathcal{B}(S)$ if there exists a constant K such that

$$\int_{-\infty}^{\infty} \|f(t)\|^2 dt \leq K \sum \|f(t_n)\|^2 \tag{32}$$

for all $f(t) \in \mathcal{B}(S)$.

We first notice that Definition 2 implies $\{t_n\}$ is also a uniqueness sequence but the converse does not hold. Definition 2 ensures that the error induced by noisy samples will be bounded if the noise is bounded; sampling on a sampling sequence is called stable sampling. Before presenting the conditions for a sampling sequence, we provide the definition of the Beurling lower density:

Definition 3: **[28], [29]** The Beurling lower density of a sequence $\{t_n\}$ is defined as

$$D_-(\{t_n\}) = \liminf_{r\to\infty} \inf_a \frac{1}{r} \sharp\{\{t_n\} \cap [a, a+r]\}. \tag{33}$$

We now can state the necessary and sufficient conditions for a sampling sequence in the following theorem that was proved in [23] :

Theorem 6: **[23]** A sequence $\{t_n\}$ is a set of stable sampling for $\mathcal{B}(S)$ if the Beurling lower density $D_-(\{t_n\})$ is at least $\frac{m(S)}{2\pi}$, where $m(S)$ is the measurement of the support of S.

In cases where there are infinite samples in the past or within a finite interval, since such samples constitute a uniqueness sequence but not a sampling sequence, a small perturbation can lead to a substantially different reconstructed signal. From Theorem 5 and 6, if the Beurling lower density is higher than the Nyquist rate, uniqueness is ensured and stable reconstruction is possible. Several reconstruction methods have been proposed under this condition. [3], [4] provided great reviews of these reconstruction methods.

APPENDIX B
PROOF OF PERFECT RECONSTRUCTION WHEN THE IASR CONVERGES

When the IASR converges, we know that the amplitude-time function of the reconstructed signal and the amplitude-time function of the original signal agree at $n\Delta$ for all n. These samples $(n\Delta, h(n\Delta))$ can be bijectively mapped to $(t_n, f(t_n))$. That is, the reconstructed signal and the original signal agree at t_n for all n. As a result, to show that when the IASR converges the reconstructed signal is identical to the original signal, it is sufficient to show that $\{t_n\}$ is a sampling sequence, which from Theorem 6 can be shown by checking if the Beurling lower density is larger than the Nyquist sampling density. A satisfaction of this requirement ensures not only perfect reconstruction but also stability.

From Section II, we know $t_n = \frac{n\Delta - f(t_n)}{\alpha}$. Finding the number of sampling between time a and time $a + r$ is equivalent to finding the number of integer n such that

$$\begin{aligned} & a \leq \frac{n\Delta - f(t_n)}{\alpha} \leq a + r. \\ \Leftrightarrow & \frac{f(t_n) + \alpha a}{\Delta} \leq n \leq \frac{f(t_n) + \alpha(a+r)}{\Delta}. \end{aligned} \tag{34}$$

Consider m such that

$$\frac{A + \alpha a}{\Delta} \leq m \leq \frac{-A + \alpha(a+r)}{\Delta}, \tag{35}$$

where A is chosen so that $-A \leq f(\cdot) \leq A$. With the choice of A, any m satisfying Eq. (35) will also satisfies Eq. (34). That is,

$$\frac{1}{r}\sharp\{\{t_m\} \cap [a, a+r]\} \leq \frac{1}{r}\sharp\{\{t_n\} \cap [a, a+r]\}. \tag{36}$$

From Eq. (35) and Eq. (36), we obtain

$$\begin{aligned} & \frac{1}{r}(\lfloor \frac{-A + \alpha(a+r)}{\Delta} \rfloor - \lceil \frac{A + \alpha a}{\Delta} \rceil + 1) \\ & \leq \frac{1}{r}\sharp\{\{t_m\} \cap [a, a+r]\} \\ \Rightarrow & \frac{1}{r}(\frac{-2A + \alpha r}{\Delta} - 1) \leq \frac{1}{r}\sharp\{\{t_m\} \cap [a, a+r]\} \\ \Rightarrow & \frac{1}{r}(\frac{-2A + \alpha r}{\Delta} - 1) \leq \frac{1}{r}\sharp\{\{t_n\} \cap [a, a+r]\} \end{aligned} \tag{37}$$

for every a and r.

We now can give a lower bound on the Beurling lower density:

$$D_-(\{t_n\}) = \liminf_{r\to\infty} \inf_a \frac{1}{r}\sharp\{\{t_n\} \cap [a, a+r]\} \geq \frac{\alpha}{\Delta}. \tag{38}$$

Therefore, if $\frac{\alpha}{\Delta} > \frac{W}{\pi}$ and if the iterative reconstruction algorithm converges, the function that the reconstruction algorithm converges to will be $f(t)$.

APPENDIX C
BACKGROUND ON THE VORONOI METHOD

In this section, we provide some background on iterative nonuniform-sampling reconstruction, in particular the Voronoi method. We first present a general technique for developing an iterative reconstruction algorithm, where we follow the discussion in [12]. Then we will show how the Voronoi method utilizes the technique. The convergence rate when the Voronoi method is applied to the amplitude sampling will then be derived.

We first state a proposition presented in [12]:

Proposition 1: **[12]** Let $\mathbf{A}$ be a bounded operator on a Banach space $(B, \|\cdot\|_B)$ such that there exists some $\gamma < 1$

$$\|f - \mathbf{A}f\|_B \leq \gamma \|f\|_B, \tag{39}$$

for all f in B. Then $\mathbf{A}$ is invertible on B and f can be recovered from $\mathbf{A}f$ by the following iteration algorithm. Setting $f_0 = 0$ and

$$f_{n+1} = f_n + \mathbf{A}(f - f_n), \tag{40}$$

we have $\lim_{n\to\infty} f_n = f$ and

$$\|f - f_n\|_B \leq \gamma^{n+1} \|f\|_B. \tag{41}$$

Notice that the linear convergence shown in Eq. (41) can be observed by rewriting Eq. (40) as $f - f_{n+1} = f - f_n - \mathbf{A}(f - f_n) = (Id - \mathbf{A})(f - f_n)$. Since from Eq. (39), we know $\|I - \mathbf{A}\| \leq \gamma$, we therefore obtain $\|f - f_{n+1}\|_B = \|(Id - \mathbf{A})(f - f_n)\|_B < \gamma \|f - f_n\|_B$. By Banach fixed point theorem [30], we have $\lim_{n\to\infty} f_n = f$ and $\|f - f_n\|_B \leq \gamma^{n+1}\|f - f_0\|_B$ which is exactly Eq. (41).

The strategy of Proposition 1 has been applied in a numerous nonuniform sampling reconstruction algorithms [31], [32]. Due to the linearity in Eq. (40), once the operator $\mathbf{A}$ is found and a parameter $\gamma < 1$ is determined to satisfy Eq. (39), this strategy is easy to be implemented; moreover, it guarantees a geometric convergence rate. To find a class of sampling spaces that are applicable to this proposition, [12] focused on the study of frames. [12] indicated that if a sequence of frames can be discovered, then $\mathbf{A}$ can be defined as the frame operator[9] and can be proved to satisfy Eq. (39). Furthermore, the convergence rate and the stability can be determined by the upper and lower frame bounds. One of the algorithms using frame operators is the Voronoi method, which was shown to be practical due to its simplicity, fast convergence rate, and robustness compared to several other iterative methods [12]. Here we provide a theorem on its convergence.

Assume that there is a nonuniform time sequence $\{t_n\}$ at which samples are obtained. We denote χ_n as the characteristic function of half interval $[t_n, t_{n+1})$; i.e. $\chi_n(t) = 1$ if $t \in [t_n, t_{n+1})$ and zero otherwise. We then obtain a zero-order hold approximation of f by $\sum_{n\in\mathbb{N}} f(t_n)\chi_n(t)$. The operator $\mathbf{A}$ is defined as the zero-order-hold approximation with a low-pass filter with a cutoff frequency the same as the bandwidth of f. That is, $\mathbf{A}f = P(\sum_{n\in\mathbb{N}} f(t_n)\chi_n(t))$ where the operator P represents the low-pass filter. With the operator $\mathbf{A}$, we can state the following theorem:

Theorem 7: **[12]** If $\delta = \sup(t_{n+1} - t_n) < \frac{\pi}{W}$ where W is the bandwidth of $f(t)$, then f is uniquely determined by its samples $f(t_n)$ and can be reconstructed iteratively as follows:

$$f_0 = Af = P(\sum_{n\in\mathbb{N}} f(t_n)\chi_n(t)). f_{k+1} = f_k + A(f - f_k). \tag{42}$$

[9]Both the definition of frames and the way to relate $\mathbf{A}$ with a frame operator can be found in [12].

Then $\lim_{n\to\infty} f_n = f$ and

$$\|f - f_k\|_B \leq (\frac{\delta W}{\pi})^{k+1}\|f\|_B. \tag{43}$$

This theorem shows that the Voronoi converges linearly with the convergence rate $r = \frac{\delta W}{\pi}$.[10] The proof of this theorem can be found in [12]. We should notice that the convergence rate is determined by the maximum time difference δ and the bandwidth W. Since δ is not the Beurling lower density (or the average sampling rate in generic cases), it is more restrictive than the requirement for a unique and stable sequence as in Theorem 6. In fact, when we apply the Voronoi method to amplitude sampling, we can derive the followings.

$$\begin{aligned} &f(t_n) + \alpha t_n = n\Delta. \\ &f(t_{n+1}) + \alpha t_{n+1} = (n+1)\Delta. \\ \Rightarrow &t_{n+1} - t_n = \frac{\Delta - (f(t_{n+1}) - f(t_n))}{\alpha}. \end{aligned} \tag{44}$$

By mean value theorem [33], there exists $\eta_n \in (t_n, t_{n+1})$ such that $f(t_{n+1}) - f(t_n) = f'(\eta_n)(t_{n+1} - t_n)$. Therefore, Eq. (44 can be rewritten as

$$\begin{aligned} &t_{n+1} - t_n + \frac{f'(\eta_n)(t_{n+1} - t_n)}{\alpha} = \frac{\Delta}{\alpha}. \\ \Rightarrow &t_{n+1} - t_n = \frac{\Delta}{\alpha}\frac{1}{1 + \frac{f'(\eta_n)}{\alpha}}. \end{aligned} \tag{45}$$

The condition for Theorem 7 to be applicable can be related to Δ as follows:

$$t_{n+1} - t_n = \frac{\Delta}{\alpha}\frac{1}{1 + \frac{f'(\eta_n)}{\alpha}} < \frac{\pi}{W}. \tag{46}$$

Notice that δ is affected by the transformation parameter α and the first derivative of the original signal f. If we choose α so that $1 + \frac{f'(\cdot)}{\alpha} > K > 0$ for some K (notice that $K < 1$ since f is not monotonic), then we require $\Delta/\alpha < \inf(1 + \frac{f'(t)}{\alpha})\frac{\pi}{W}$ for the Voronoi method to be applicable, while we only require $\Delta/\alpha < \frac{\pi}{W}$ for the corresponding time sequence $\{t_n\}$ to be a sampling sequence.

REFERENCES

[1] C. E. Shannon, "Communication in the presence of noise," *Proc. IRE*, vol. 37, pp. 10–21, 1949.

[2] A. D. Wyner and S. Shamai, "Introduction to 'communication in the presence of noise' by c. e. shannon," *Proc. IEEE*, vol. 86, pp. 442–226, Feb. 1998.

[3] M. Unser, "Sampling-50 years after shannon," *Proc. IEEE*, vol. 88, no. 4, pp. 569–587, Apr. 2000.

[4] J. L. Yen, "On nonuniform sampling of bandwidth-limited signals," *Circuit Theory, IRE Transactions on*, vol. 3, no. 4, pp. 251–257, Dec. 1956.

[5] J. W. Mark and T. D. Todd, "A nonuniform sampling approach to data compression," *IEEE Trans. Commun.*, vol. 29, no. 1, pp. 24–32, 1981.

[6] Jr. B. F. Logan, "Information in the zero crossings of bandpass signals," *AT&T Technical Journal*, vol. 56, pp. 487–510, Apr. 1977.

[7] P. T. Boufounos and R. G. Baraniuk, "Reconstructing sparse signals from their zero crossings," in *Acoustics, Speech and Signal Processing, 2008. ICASSP 2008. IEEE International Conference on*, Mar. 2008, pp. 3361–3364.

[8] N. Sayiner, H. V. Sorensen, and T. R. Viswanathan, "A level-crossing sampling scheme for a/d conversion," *IEEE Trans. Circuits Syst. II, Analog Digit. Signal Process.*, vol. 43, no. 4, pp. 335–339, Apr. 1996.

[9] E. Allier, G. Sicard, L. Fesquet, and M. Renaudin, "A new class of asynchronous a/d converters based on time quantization," *Proc. 9th IEEE Int. Symp. Asynchronous Circuits Syst.*, pp. 196–205, 2003.

[10] B. Schell and Y. Tsividis, "A continuous-time adc/dsp/dac system with no clock and with activity-dependent power dissipation," *IEEE J. Solid-State Circuits*, vol. 43, no. 11, pp. 2472–2481, Nov. 2008.

[11] P. Martnez-Nuevo, "Amplitude sampling for signal representation," *Doctoral Thesis*, Aug. 2016.

[12] H. G. Feichtinger and K. Grchenig, "Theory and practice of irregular sampling," *Wavelets: mathematics and applications*, pp. 305–363, 1994.

[13] M. Hazewinkel, "Composite function," *Encyclopedia of Mathematics*.

[14] A. Quarteroni, F. Saleri, and P. Gervasio, "Scientific computing with matlab and octave," *Springer*, 2010.

[15] H. Jeffreys and B. S. Jeffreys, *Methods of Mathematical Physics, 3rd ed.*, 1988.

[16] L. N. Trefethen, *Finite Difference and Spectral Methods for Ordinary and Partial Differential Equations*, unpublished text, available at http://people.maths.ox.ac.uk/trefethen/pdetext.html, 1996.

[17] S. Lang, *Complex Analysis*, Springer, 1999.

[18] G. Plya, "On an integral function of an integral function," *Journal London Mathematical Society*, vol. 1, pp. 12–15, 1926.

[19] S. M. Nikolskii, *Approximation of Functions of Several Variables and Imbedding Theorems*, Springer, 1975.

[20] H. Lai, "Reconstruction methods for level-crossing sampling," *Master's Thesis*, Jun. 2016.

[21] P. Martnez-Nuevo, H. Y. Lai, and A. V. Oppenheim, "Amplitude sampling," pp. 17–22, Sept 2016.

[22] H. Y. Lai, P. Martnez-Nuevo, and A. V. Oppenheim, "An iterative reconstruction algorithm for amplitude sampling," pp. 4576–4580, March 2017.

[23] H. J. Landau, "Sampling, data transmission, and the nyquist rate," *Proceedings of the IEEE*, vol. 55, no. 10, pp. 1701–1706, Oct. 1967.

[24] A. S. Bandeira, "Sampling and interpolation," *Relax and Conquer*, Sep. 20th 2010.

[25] H. S. Black, *Modulation Theory*, New York: van Nostrand, 1953.

[26] F. Marvasti, *Nonuniform Sampling - Theory and Practice*, Kluwer Academic/ Plenum Publishers, 2001.

[27] F. J. Beutler, "Error free recovery of signals from irregular samples," *SIAM Rev.*, pp. 8:322–335, July 1966.

[28] H. J. Landau, "Necessary density conditions for sampling and interpolation of certain entire functions," *Acta Mathematica*, vol. 117, no. 1, pp. 37, 1967.

[29] L. Carleson, P. Malliavan, J. Neuberger, and J. Wermer, *The collected works of Arne Beurling*, Birkhauser, 1989.

[30] A. Granas and J. Dugundji, *Fixed Point Theory*, Springer, New York, 2003.

[31] R. R. Coifman and R. Rochberg, *Representation theorems for holomorfic and harmonic functions in L^p*, Asterisque 77, 1980.

[32] K. Grochenig, *Describing functions: atomic decompositions versus frames*, Monatsh. Math, 1991.

[33] M. Hazewinkel, "Cauchy theorem," *Encyclopedia of Mathematics*.

[10] A sequence $\{x_k\}$ is said to have a linear convergence rate r if $\lim_{k\to\infty} \frac{\|x_{k+1} - x^*\|}{\|x_k - x^*\|} = r$ where $\lim_{k\to\infty} x_k = x^*$. Therefore, the sequence converges faster as the convergence rate $r \to 0$.